Evaluation of Sediment Yield and Risk Management of Sediment Disaster With the Natural Resources Conservation Service-Curve Number Method

Wen-Yan Zhang[1]

[1]National Chung Hsing University

February 10, 2021

Abstract

Subtropical areas are often struck by typhoons. The sediment disasters that accompany typhoons severely affect the environment. However, sediment yield (SY) data usually lack integrity. This study used long-term daily river discharge and SY data to establish a runoff–SY rating curve (Q–Qs rating curve) and used it to estimate the SY of typhoon events. In addition, based on the curve number, this study analyzed the relationship between the potential maximum retention (S) and SY; the results showed that different amounts of cumulative rainfall correspond to different S–SY functions; thus, the potential maximum erosion (A) of the catchment area could be estimated using this characteristic. For a sediment management strategy, this study took subdivisions as a unit and incorporated the potential maximum erosion (A) and slope to establish a map indicating the spatial distribution of sediment disaster risks. To determine the priority areas for management, the relationship between the cumulative number of subdivisions and landslide rate could be used to determine the areas with high potential, which can serve as a reference for related management research.

1. INTRODUCTION

Although science and technology continue to progress, the world is still severely affected by natural disasters. Numerous studies have explored the mechanism of natural disasters (Shuin, Hotta, Suzuki, & Ogawa, 2012; Oku & Nakakita, 2013; Zanandrea, Michel, Kobiyama, & Cardozo, 2019; Nam, Kim, Kang, & Kim, 2019); however, factors affecting disasters are complex. In addition to the environmental condition of the catchment area, anthropogenic activity is a prominent factor. Taiwan, an island surrounded by ocean, is no exception; moreover, Taiwan faces the threat of natural disasters because of its geographical location. The climate is affected by the monsoon throughout the year, mainly the northeast monsoon prevailing from mid-October to April of the following year and the southwest monsoon prevailing from mid-June to September. Specifically, July to September is the typhoon season (Kuo, Lee, & Lu, 2016), and during this period, three to four typhoons striking Taiwan is common. Rainfall during the passage of typhoons is characterized by its long duration and high intensity; such rainfall patterns often cause severe disasters (Yang et al., 2011; Milliman, Lee, Huang, & Kao, 2017).

To mitigate disasters during the passage of typhoons, experiential and physical models have been developed by several studies and can be used to analyze the processes of disaster occurrence (Chen, Jhong, Wu, & Chen, 2013; Yang et al., 2015). Specifically, experiential models can be used to obtain data in a short time; however, this type of model requires a large amount of observational data, and thus is time-consuming. Physical models are usually developed based on a fine theoretical foundation; however, the parameters are usually overly complex. Therefore, both model types have advantages and disadvantages. After the United States (US) government passed the Flood Control Act of 1936, numerous American hydrologists vigorously developed rainfall-runoff models. Finally, in 1956, the US Soil Conservation Service (now Natural Resources

Conservation Service) developed the curve number (CN) method, which has been widely applied to simulate or predict runoff from rainfall (Huang, Gallichand, Wang, & Goulet, 2006; Ali, Khan, Aslam, & Khan, 2011; Deshmukh, Chaube, Hailu, Gudeta, & Kassa, 2013; Lal, Mishra, & Pandey, 2015; Ozdemir & Elbaşı, 2015).

Sediment yield (SY) information is essential for environmental and flood control; thus, catchment survey projects usually require it as a reference for catchment planning and design. In the 1960s, a model for assessing SY was developed in response to the need for environmental management (Wischmeier & Smith, 1965). The model effectively simplified the calculation of catchment areas by using natural empirical parameters, and it can be applied to estimate SY during rainstorms or throughout the year. In recent decades, numerous models have been developed to simulate SY, including the universal soil loss equation, revised universal soil loss equation, and modified universal soil loss equation (Chandramohan, Venkatesh, & Balchand, 2015; Furl, Sharif, & Jeong, 2015; Zerihun, Mohammedyasin, Sewnet, Adem, & Lakew, 2018). For the conservation of soil and water resources in catchment areas, runoff and SY are crucial information; thus, studies have used the CN method to estimate the SY in catchment areas (Mishra, Tyagi, Singh, & Singh, 2006; Gajbhiye, Mishra, & Pandey, 2014). In addition to providing runoff information, the CN method can be used to estimate SY.

Although hydrological and SY models have been well established, they require high-quality input data, which are difficult to acquire from long-term monitored catchment areas. Therefore, this study sought to estimate the SY of a catchment area by using big data and the CN method. In addition, the conservation of soil and water resources in a catchment area is essential; thus, this study proposed a hierarchical sediment risk management method based on the concept of subdivisions management and established a management mechanism to serve as a reference for future disaster management.

2. MATERIALS AND METHODS

This study used rainfall, runoff, and SY data to establish a relational curve between the potential maximum retention (S) and SY. Land use and soil data were incorporated with the S–SY curve to estimate the spatial distribution of the potential maximum erosion. Finally, a digital elevation model (DEM) was used to determine the subdivision delineation, and the top-priority management area (Figure 1) was selected based on the potential maximum erosion and slope of each unit area.

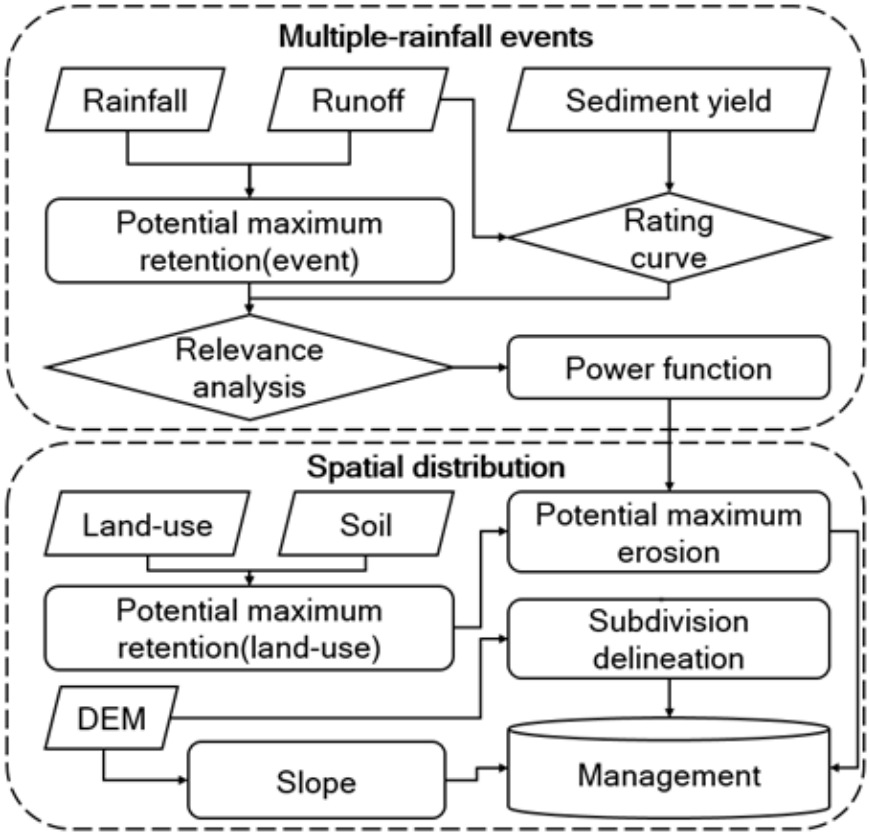

Figure 1. Research procedure.

2.1 Study Area

The study area was in the catchment area of the Chenyulan River (23°20'–23°35' N, 120°47'–121°00' E) (Figure 2), which is a tributary of the Zhuoshui River basin in central Taiwan; its catchment area is approximately 448 km^2 and the river's length is approximately 42 km. Based on hydrological data, the annual average temperature in this area is 19–23°C and the annual average rainfall is 1600–2600 mm. Regarding the topography, the catchment area of the basin is narrow and elongated. The main stream flows northward and the tributaries flow into the main stream from the east and west. In terms of geology, the left bank of the river is mostly Middle Miocene sedimentary rock and the right bank is Paleogene slate. The topography of the main stream is a linear longitudinal valley (Lee, 1996).

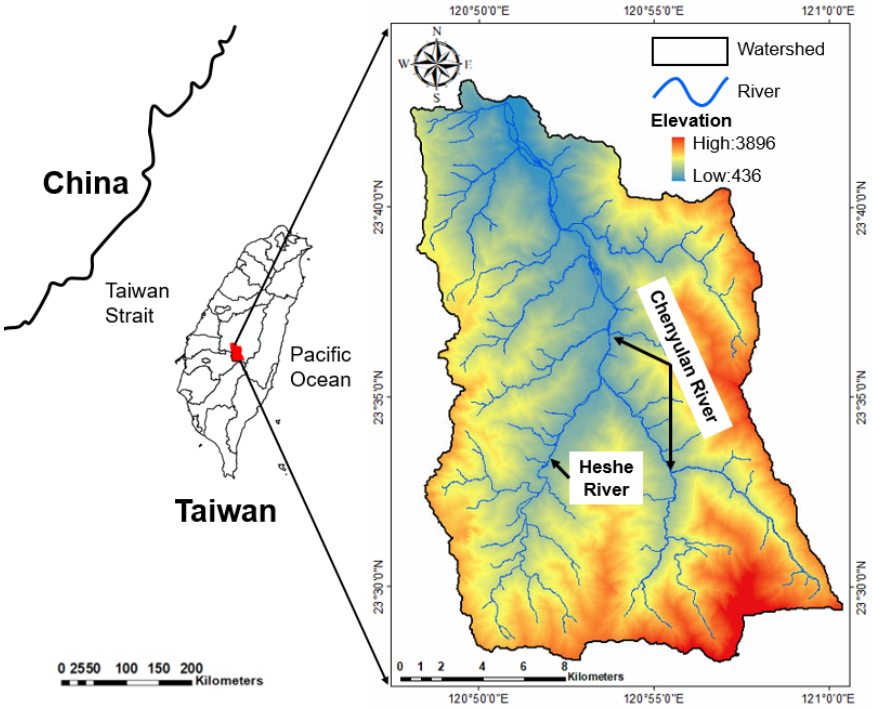

Figure 2. Location of the study area and a topographic map.

2.2 Study Materials

Table 1 lists information about the study materials. Land use was classified using survey data from the National Land Surveying and Mapping Center. Soil maps from the Soil and Water Conservation Bureau were used to determine the hydrologic soil groups. Furthermore, the spatial distribution of CN values was estimated using land use and the hydrologic soil groups. Rainfall, flow rate, and SY data were acquired from the observational data of the Water Resources Agency, Ministry of Economic Affairs as a reference for long-term analysis and verification. In addition, DEM was used to determine the subdivision delineation of the catchment area.

Table 1. Study materials.

Map/ Information	Year	Resolution	Source	Application
Land-use	2008	1/5000	National Land Surveying and Mapping Center	To calculate CN
Soil	2005	1/5000	Soil and Water Conservation Bureau	To calculate CN
Rainfall	1999~2009	Daily data	Water Resources Agency	Estimation of Direct runoff
Runoff	1999~2009	Daily data	Water Resources Agency	Model Verification
Sediment yield	1999~2009	Daily data	Water Resources Agency	Model Verification

Map/ Information	Year	Resolution	Source	Application
DEM	2004	5m*5m	Department of Land Administration	To Delineate watersheds

2.3 Methodology

The research method comprised five parts: (1) the natural resources conservation service -CN (NCRS-CN) method, (2) land use and soil, (3) SY model, (4) typhoon event analysis, and (5) management practices. Details of these parts are introduced in the following sections.

2.3.1 NCRS-CN Method

The NCRS-CN method is widely used to determine the relationship between rainfall and runoff and can be applied to study areas with insufficient data. This is because the primary input parameters of this method are land use and soil type, which are usually available and readily acquired. Furthermore, land use and soil type data can be collected from public survey data provided by government agencies. The NCRS-CN method was developed by the Natural Resources Conservation Service in the US. It was established based on a water balance equation and two fundamental hypotheses. The first assumption is that the ratio of direct surface runoff and potential maximum surface runoff equals the ratio of infiltration and potential maximum retentions. The second assumption is that the initial abstraction is part of the potential maximum retention. The formulas expressing the relationship between rainfall and runoff in the NCRS-CN method are as follows:

$Q = 0, P < 0.2S \ldots$ (1)

$Q = (P - 0.2S)^2/(P + 0.8S), P > 0.2S \ldots$ (2)

where Q is the direct runoff depth (mm); P is the rainfall depth (mm); and S represents the potential maximum retention (mm). The relationship between S and CN can be expressed as

$S = (25400/CN) - 254 \ldots$ (3)

The formula for estimating the average CN of a catchment area is

$CN_{av} = [?]\ (A_i \times CN_i)/[?]A_i \ldots$ (4)

where CN_{av} is the average CN of the catchment area; A_i represents the grid area (m2); and CN_i is the CN of the grid.

2.3.2 Land Use and Soil

Land use is an essential input factor for the NCRS-CN method. Survey data from 2008 provided by the National Land Surveying and Mapping Center were used as a reference for land use classification (Figure 3). The percentages of land use area in the Chenyulan River catchment area are as follows: buildings (1.1%), coniferous forest (14.0%), water body (0.4%), upland field (3.0%), wasteland (9.7%), broadleaf forest (13.9%), orchard (5.6%), and other forest (52.2%). In addition, the hydrologic soil groups could be classified according to soil data (Figure 4); the classification results indicated that the catchment area was primarily composed of B and D Groups.

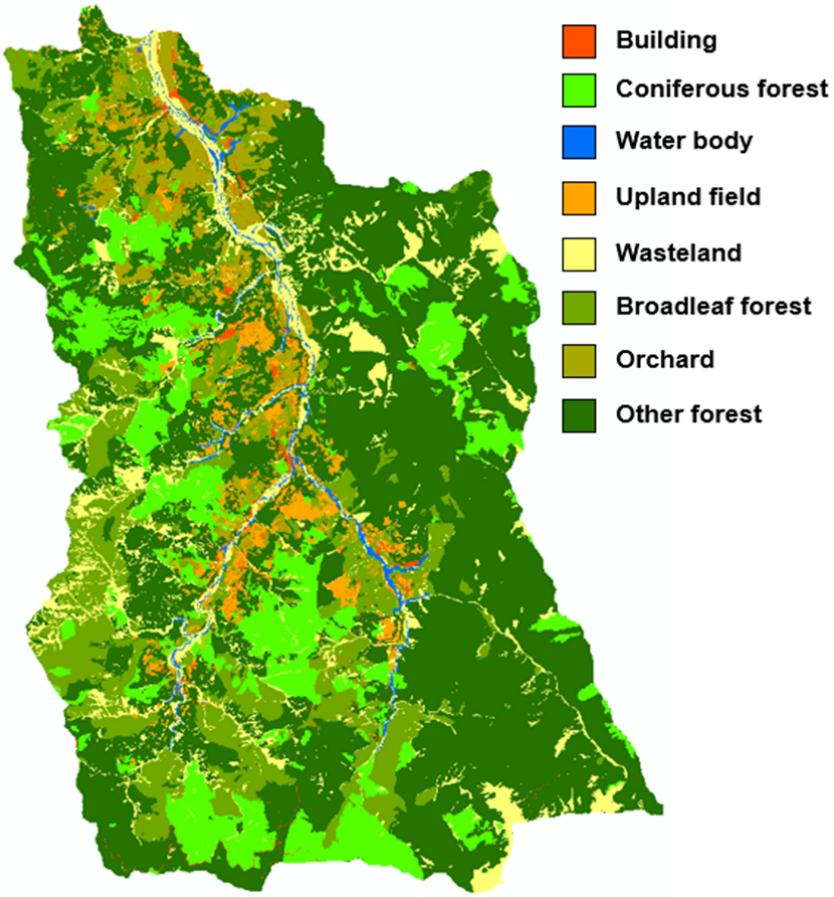

Figure 3. Land use of the study area.

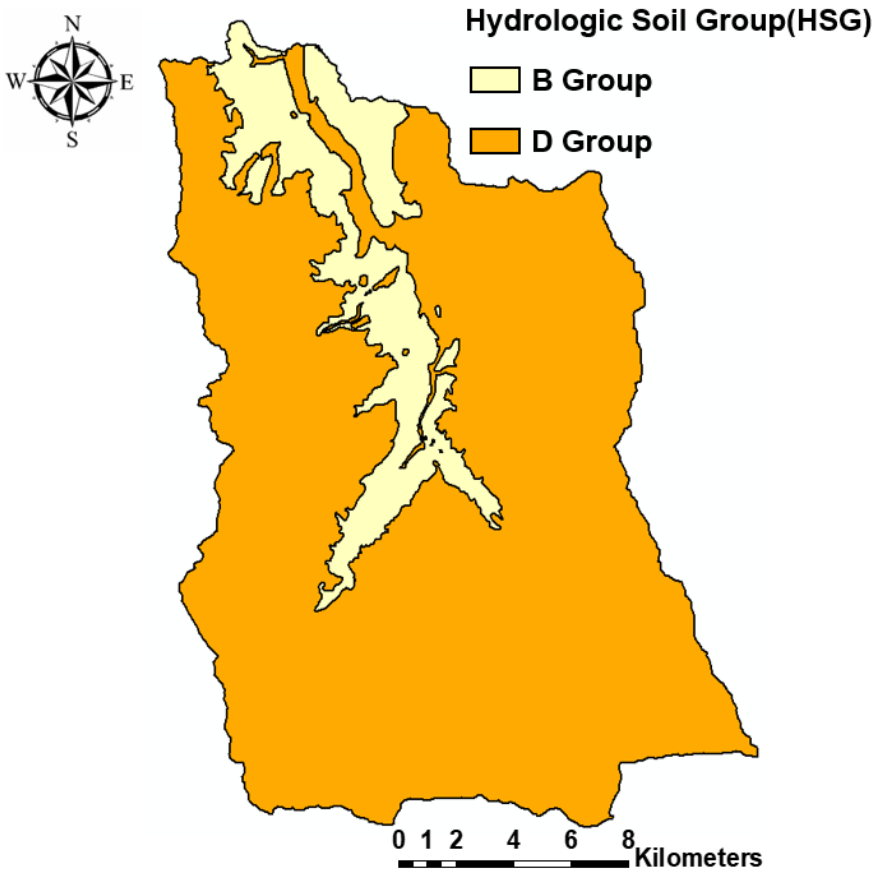

Figure 4. Hydrologic soil groups of the study area.

2.3.3 Sediment Yield Model

Numerous studies have used the NCRS-CN method to estimate SY (Mishra, Tyagi, Singh, & Singh, 2006; Gajbhiye, Mishra, & Pandey, 2014). It can effectively improve estimation efficiency and overcome the problem of inadequate data in some areas. This method's formula is as follows:

$$C = Q/P = F/S = P/(P + S) = (SY)/A \ldots \quad (5)$$

where C is the runoff coefficient; Q is the direct runoff depth (mm); P is the rainfall depth (mm); F is cumulative infiltration (mm); S is the potential maximum retention (mm); SY is the actual sediment yield (mm); and A is the potential maximum erosion (mm).

The characteristics of the catchment area, including A, P, and S, would affect the SY. Increasing the runoff would increase the volume of sediment erosion and transportation, and may result in an increase in SY. The formula is as follows:

$$SY = AP/(P + S) \ldots \quad (6)$$

In Eq. (6), S and SY are in inverse proportion. If S approaches 0, SY would approach A. Sediment erosion is affected by runoff; thus, SY and S are correlated. The formula is as follows:

$$SY = a(S)^{-b} \ldots \quad (7)$$

where a is a coefficient and b is the exponent.

2.3.4 Typhoon Event Analysis

To investigate the relationship between rainfall and SY, this study explored the process of rainfall events. The concepts of runoff analysis and SY estimation can be explained by taking the rainfall events between August 16 and September 13, 2007 as examples (Figure 5). The details are as follows: (1) For the rainfall analysis, four rainfall stations were present in the catchment area; thus, the Thiessen polygons method was used for estimation. (2) For the runoff analysis, because this study investigated the runoff produced by rainfall events, the straight line analysis was adopted to deduct the base flow. (3) A rating curve was used to estimate SY. Rainfall events (Figure 5) indicated that the values of cumulative rainfall, cumulative runoff, and cumulative SY were 684.1, 487.6, and 9.6 mm, respectively. In addition, the potential maximum retention could be estimated using the cumulative rainfall and cumulative runoff in rainfall events, and the value was 205.0 mm.

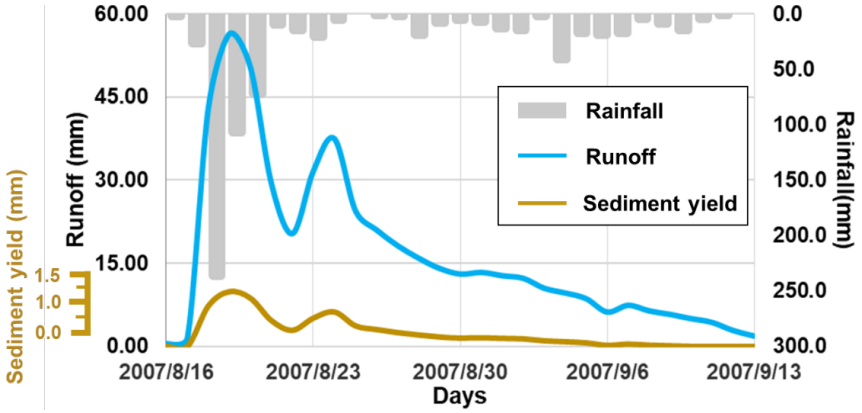

Figure 5. Observational data of typhoon events.

2.3.5 Management Practices

2.3.5.1 Subdivision of the Management Area

To explore the management strategy of sediment in the catchment area, this study divided the catchment area into multiple subdivisions to facilitate the determination of essential areas within it. Catchment area division was based on two concepts—the establishment of a depressionless flow direction (Jenson & Domingue, 1988) and the establishment of gridded cumulative discharge (O'Callaghan & Mark, 1984). After the threshold values of each subdivision were determined, the division of the catchment area would automatically be conducted. Based on this principle, the Chenyulan River catchment area could be divided into 269 subdivisions (Figure 6).

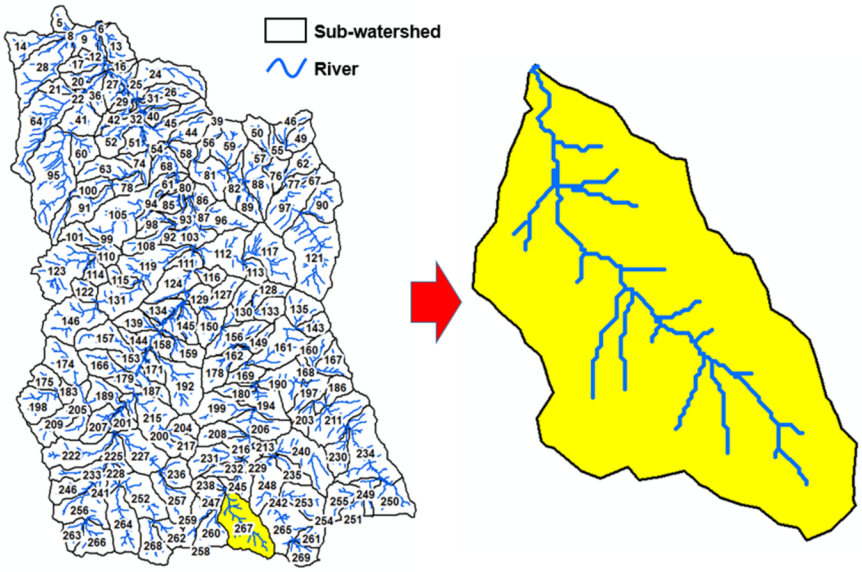

Figure 6. Subdivisions of the Chenyulan River catchment area.

2.3.5.2 Slope

Studies have shown that natural factors such as climate, land cover pattern, topography, geology, and soil characteristics affect soil erosion (Vrieling, 2006; Shin, Park, Pierson, & Williams, 2019). This study incorporated the CN method, potential maximum retention, and SY to estimate the potential maximum erosion of the catchment area. This method considered climate, land cover pattern, geology, and soil characteristics but did not consider topography. Therefore, this study established the average slope of each subdivision based on the DEM to correct the model.

3. RESULTS

3.1 Runoff and Sediment Yield

To investigate the temporal relationship between runoff and SY, this study used observational data of the Water Resources Agency, Ministry of Economic Affairs during 1999–2009 to plot the temporal distribution of runoff and SY (Figure 7) and display the daily runoff and SY values. Figure 7 shows that the peaks of runoff and SY occurred mostly during July–October, and mainly in the typhoon season in Taiwan. The maximum daily runoff and maximum daily SY occurred during Typhoon Morakot (August 8, 2009), and the values were 228.55 and 10.35 mm, respectively.

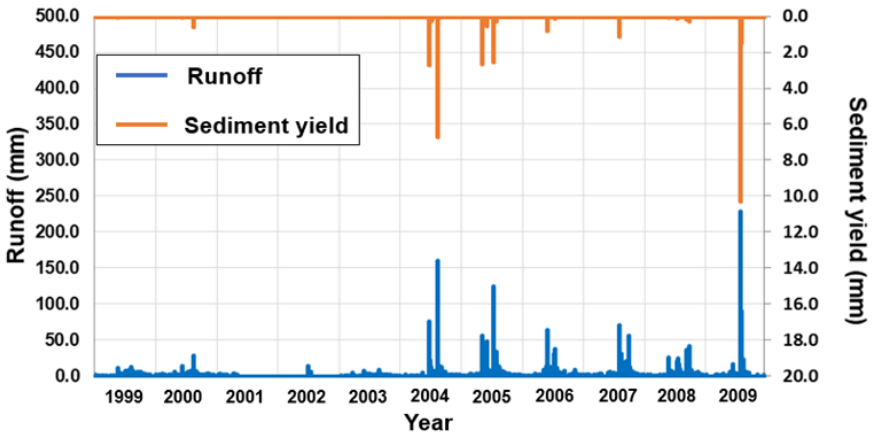

Figure 7. Temporal distribution of runoff and SY during 1999–2009.

Daily runoff and SY data were used to establish the rating curve (Q–Qs rating curve; Figure 8). The correlation coefficient was 0.95 as determined using regression analysis. The curve ($Y = 0.0002x^2 + 0.0046x$) could be used to estimate event-based SY.

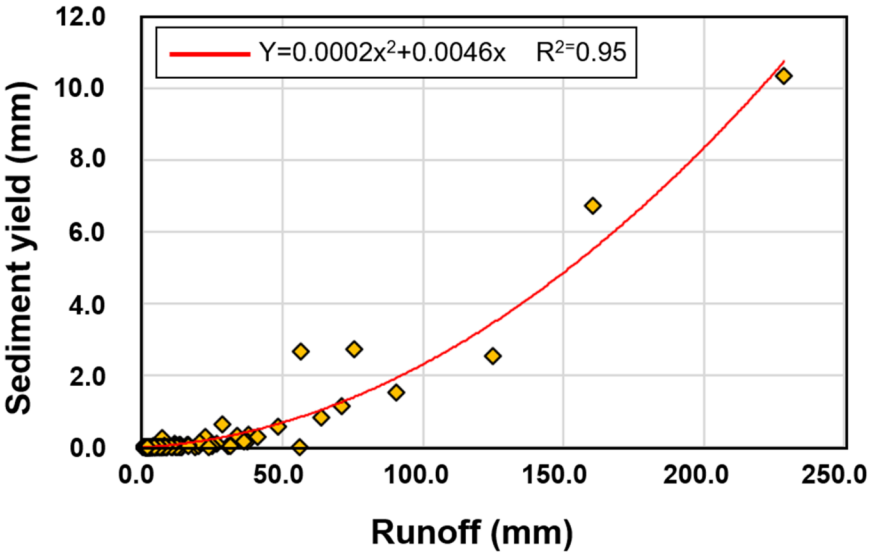

Figure 8. Rating curve of runoff and SY.

3.2 Potential Maximum Retention and Sediment Yield

Potential maximum retention was an essential parameter in the calculation of CN values. These calculations considered rainfall, runoff, and initial loss and were widely applied to estimate runoff from rainfall data. If the potential maximum retention could be used to estimate SY, then the relationship between the two parameters could serve as a reference for management strategies. Therefore, this study analyzed typhoon events during 1999–2009 to investigate the relationship between potential maximum retentions and SY.

Based on a study of rainfall events (Gajbhiye, Mishra, & Pandey, 2014), the relationship between the two parameters could be expressed by a power function. The two curves in Figure 9 exhibit similar trends; however, this study found that different cumulative rainfall conditions should be classified and investigated

individually. The two functions in Figure 9 were suitable for high cumulative rainfall ($SY=13764S^{-1.133}$) and low cumulative rainfall ($SY = 473.64S^{-0.866}$), and the correlation coefficients were 0.92 and 0.71, respectively.

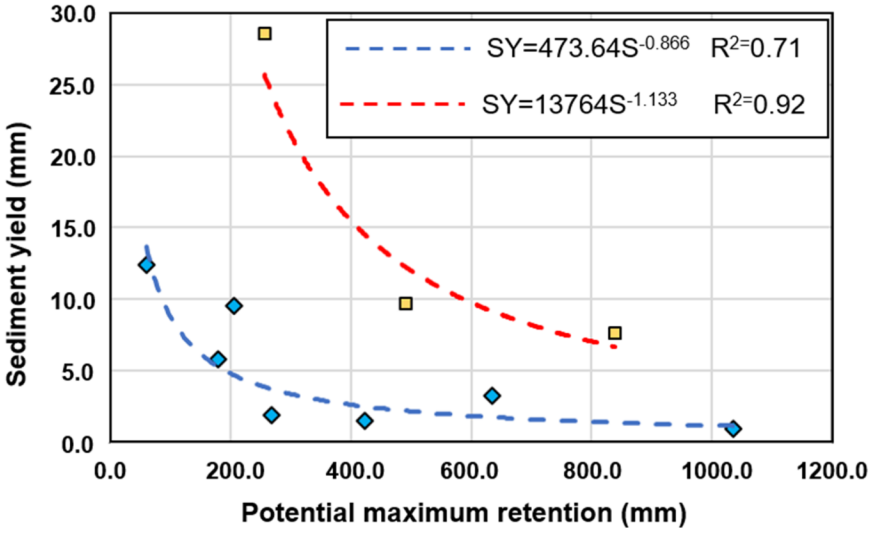

Figure 9. Relationship between potential maximum retention and SY during a typhoon event.

The observational data showed that the two parameters would exhibit different functional relations under different cumulative rainfall conditions. The functional relationships could be divided into three types according to the cumulative rainfall value, namely Type I—cumulative rainfall value < the invoked value of SY; Type II—cumulative rainfall value > the invoked value of SY, which was classified as low cumulative rainfall ($SY = 473.64S^{-0.866}$); and Type III was classified as high cumulative rainfall ($SY = 13764S^{-1.133}$).

Table 2 lists the applicable functions for expressing the relationship between cumulative rainfall and SY recorded in typhoon events during 1999–2009. According to the data, Type I cumulative rainfall was < 197.2 mm, and typhoon events classified into this category were Maggie (June 1999), Soudelor (June 2003), Nanmadol (December 2004), Longwang (September 2005), and Parma (October 2009). Type II covered the range from 197.2 to 754.4 mm, and corresponding typhoon events were Bilis (June 1999), Haitang (July 2005), Bilis (July 2006), Sepat (August 2007), Krosa (October 2007), Kalmaegi (July 2008), and Fung-Wong (July 2008). Type III covered the range from 754.4 to 1419.7 mm, with the corresponding typhoon events being Mindulle (June 2004), Sinlaku (September 2008), and Morakot (August 2009).

Table 2. Cumulative rainfall in typhoon events and applicable functions.

TYPE	Accumulative Rainfall(mm)	Function	R^2
Type I	<197.2	-	-
Type II	197.2~754.4	$SY=473.64S^{-0.866}$	0.71
Type III	754.4~1419.7	$SY=13764S^{-1.1330}$	0.92

3.3 Potential Maximum Retention and Erosion

Estimation of CN values is crucial for analyzing retention and SY; thus, this study used a geographic information system to integrate land use and hydrologic soil group data to estimate the spatial distribution of CN values (Figure 10). The higher the CN value, the greater the potential of the runoff in a location, and vice versa. Figure 10 shows that relatively high CN values were mostly distributed in water bodies, buildings, wasteland, and upland fields.

In addition, the spatial distribution of CN values could be incorporated into Eq. (3) to estimate the potential maximum retention. Figure 11 shows that areas with relatively large retention values were distributed in forests, indicating that forest areas exhibited favorable retention potential. The analytical results of the curves of potential maximum retention and SY showed that the curves could be divided into two types according to the cumulative rainfall. For high cumulative rainfall, $SY=13764S^{-1.133}$ was applicable, whereas for low cumulative rainfall, $SY=473.64S^{-0.866}$ was. Equation (6) could be used to estimate the spatial distribution of the potential maximum erosion volume (A) in the two aforementioned scenarios (Figure 12). Figure 12 shows the spatial distribution of potential maximum erosion values under cumulated rainfall ranges of (a) 197.2–754.4 mm and (b) 754.4–1419.7 mm.

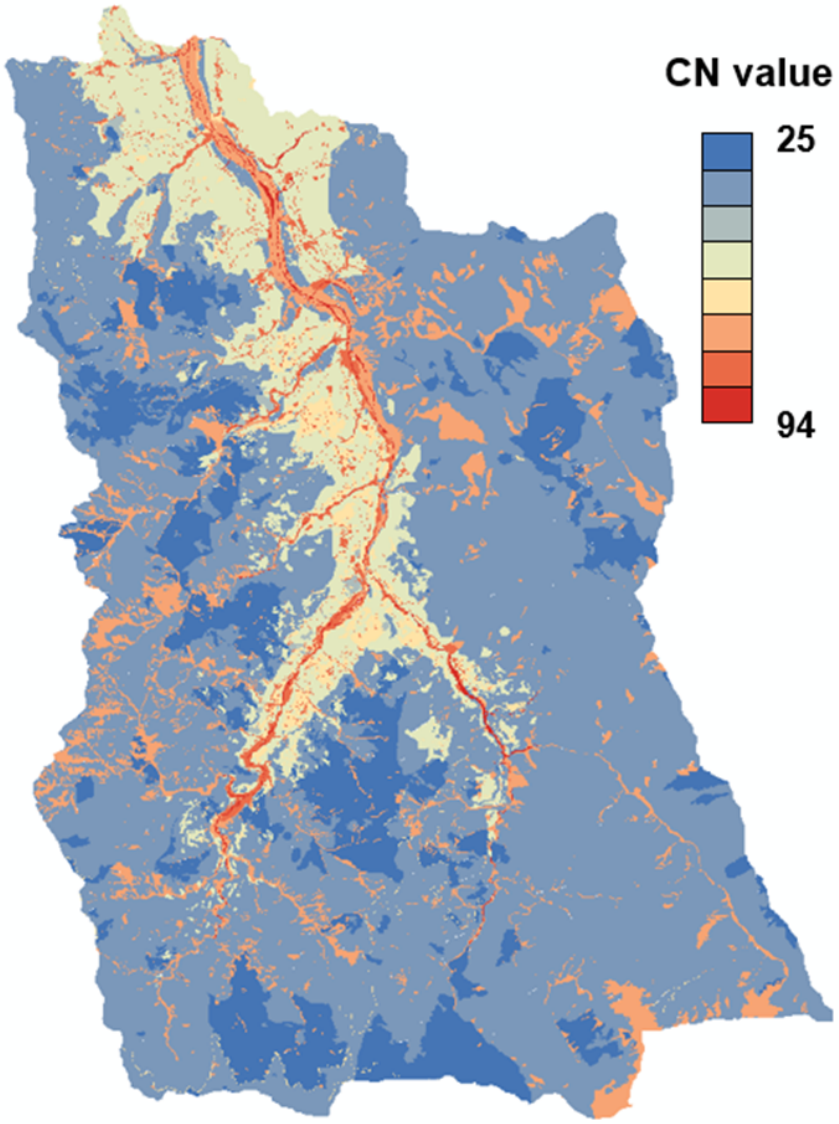

Figure 10. Spatial distribution of CN values.

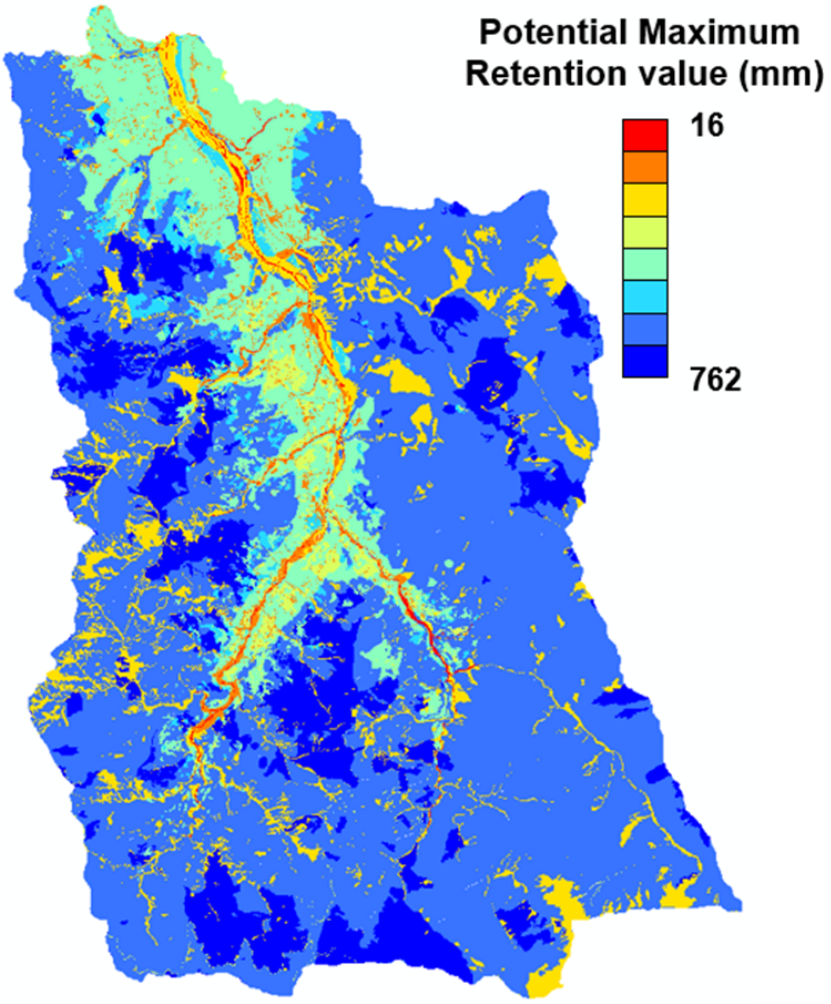

Figure 11. Spatial distribution of Potential Maximum Retention values.

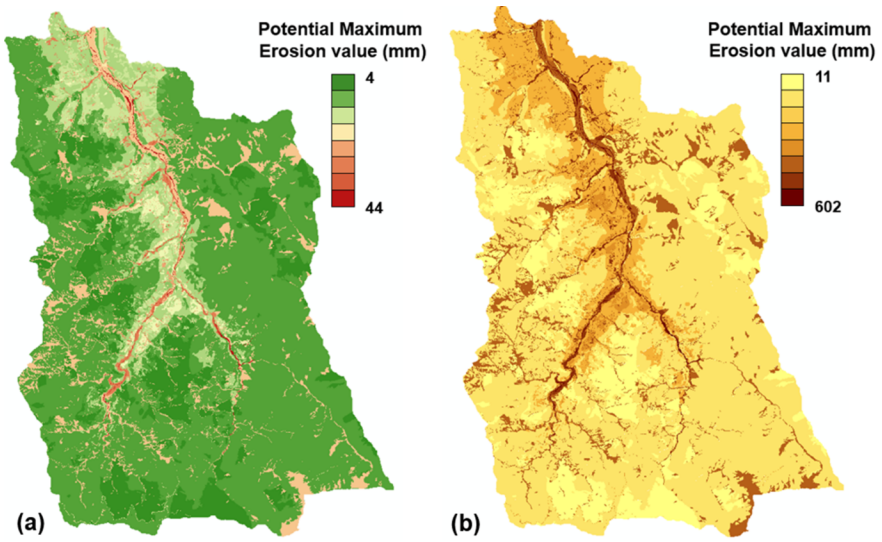

Figure 12. Spatial distribution of Potential Maximum Erosion values: (a) Type II and (b) Type III.

4. DISCUSSIONS

To investigate the relationship between the potential maximum retention and SY in the Chenyulan River catchment area in typhoon events during 1999–2009, the rating curves of the runoff and SY were first established. Rating curve analysis results showed that the two parameters were positively correlated ($Y = 0.0002x^2 + 0.0046x$), and the correlation coefficient reached 0.95. Therefore, the rating curve is applicable for estimating SY in rainfall events.

The relationship between the potential maximum retention and SY indicated that first, the relationship of the two parameters conformed to a power function, which was consistent with the aforementioned study on rainfall events (Mishra, Tyagi, Singh, & Singh, 2006). Second, the event-based cumulative rainfall was the primary cause of the difference in functions, which was different from relevant studies, and thus this study categorized cumulative rainfall into three scenarios. Type I cumulative rainfall was less than 197.2 mm, which was smaller than the invoked value of SY; Type II was 197.2–754.4 mm, and the corresponding function was $SY = 473.64S^{-0.866}$; and Type III was 754.4–1419.7 mm, and the corresponding function was $SY = 13764S^{-1.133}$.

The difference in S–SY curves of Types II and III was primarily caused by cumulative rainfall. Different cumulative rainfall levels affected the relationship between the potential maximum retention and actual SY. For Type II, the cumulative rainfall was slightly higher than the invoked SY value; thus, the S–SY curve was relatively flat. For Type III, because of higher cumulative rainfall level, according to the concept of energy accumulation, the same condition for S would cause a relatively large SY; therefore, the S–SY curve was relatively steep. In addition, the difference in S–SY curves can also be explained by the infiltration rate decreasing over time. When the duration of rainfall is long, high cumulative rainfall would easily cause soil saturation, thereby inducing more surface runoff and soil erosion.

To facilitate sediment management in the catchment area and effectively determine key locations, this study took each subdivision as a unit. The average potential maximum erosion and average slope of each subdivision were considered to determine the subdivisions with top management priority. If the average potential maximum erosion was larger and the corresponding slope was steeper, sediment disasters would be more likely to occur in such an area. Therefore, such regions should be prioritized for management. The average potential maximum erosion of the subdivisions could be estimated by the S–SY function (Figure 13(a)), whereas the subdivision slope could be extracted using the DEM (Figure 13(b)). Through the normalization

of the two parameters, the risk of sediment disasters in each subdivision could be estimated (Figure 13(c)), and the higher the risk value, the higher the priority that should be assigned to that subdivision.

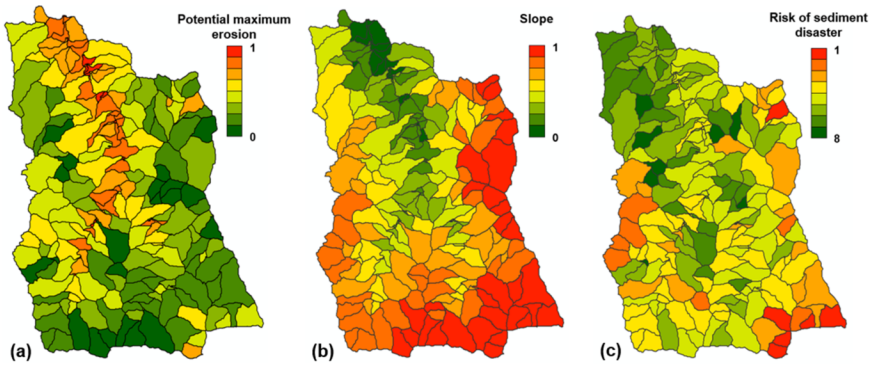

Figure 13. Spatial distributions of (a) potential maximum erosion, (b) slope, and (c) risk of sediment disaster in the catchment area.

The risk of sediment disasters in the Chenyulan River catchment area could be determined using the potential maximum erosion and slope. To explore the difference between analytical results and the actual situation, actual landslide data were investigated. This study ranked the risk of sediment disaster of 269 subdivisions from largest to smallest, and the first 1, 5, 10, 20, 40, 60, 80, 100, 120, 140, 160, 180, and 196 subdivisions were extracted to estimate their landslide rates (cumulative landslide area of the subdivision/total landslide area in the catchment area). Figure 14 shows that in the top 20 subdivisions, the cumulative landslide area accounted for 40.1% of the total landslide area in the catchment area. For the top 196 subdivisions, the cumulative landslide area accounted for 100% of the total landslide area in the catchment area. The results indicated that the cumulative number of subdivisions was positively correlated with the landslide rate. In areas with limited data, the relational curve between the cumulative number of subdivisions and landslide rate could be used to determine subdivisions with management priorities. This study investigated the number of subdivisions and their spatial distribution in a 70% landslide rate scenario; Figure 14 shows that the number of subdivisions corresponding to this rate was 80. Figures 15 and 16 indicate that the results between the selected subdivisions and actual landslides were mostly consistent.

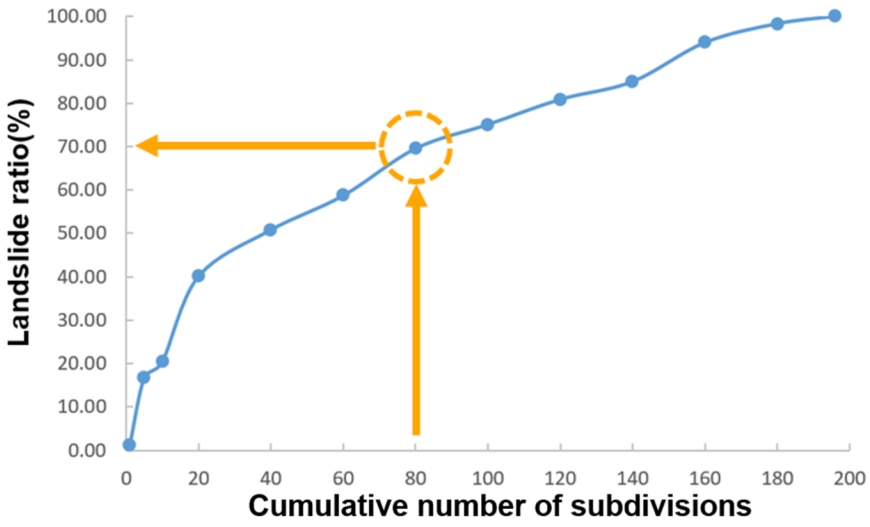

Figure 14. Relationship between the cumulative number of subdivisions and landslide rate.

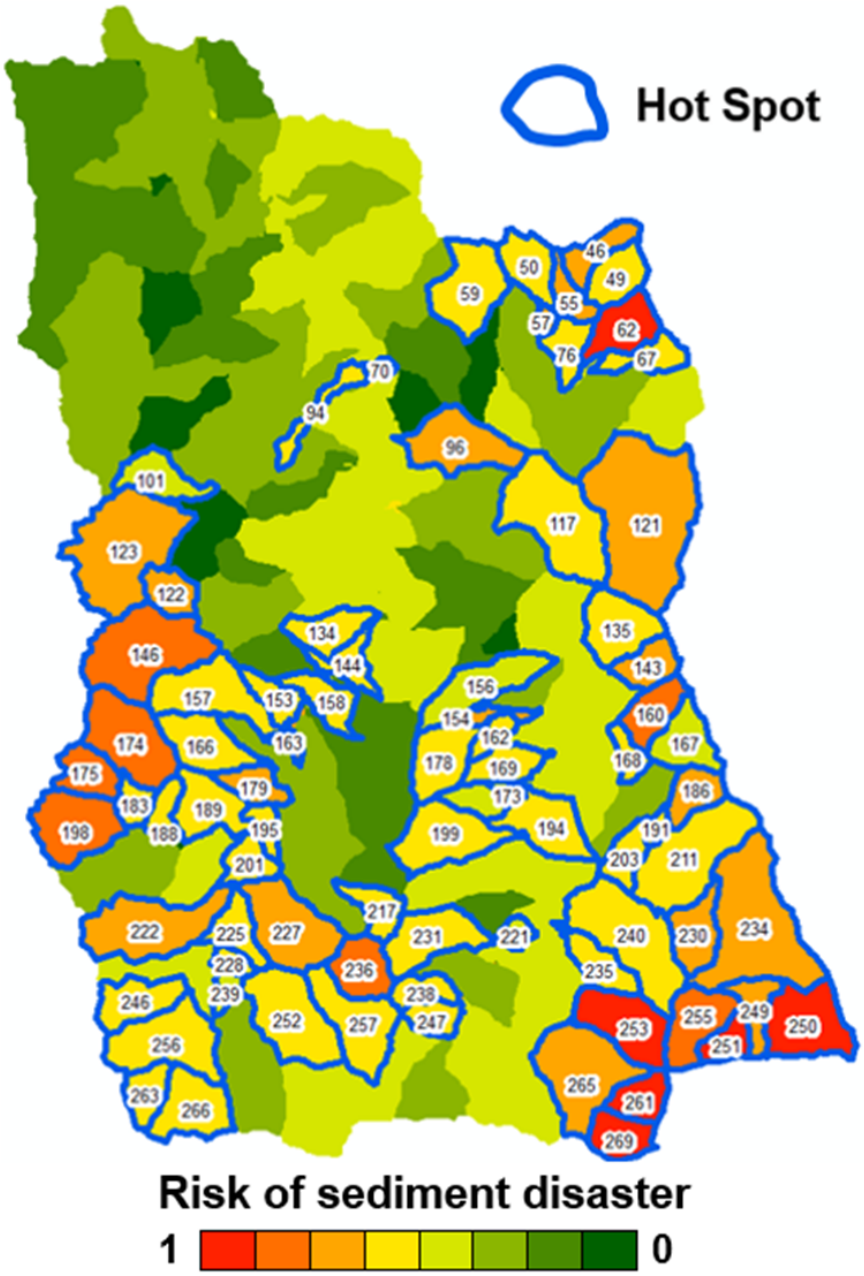

Figure 15. Spatial distribution of the risk of sediment disaster in the catchment area.

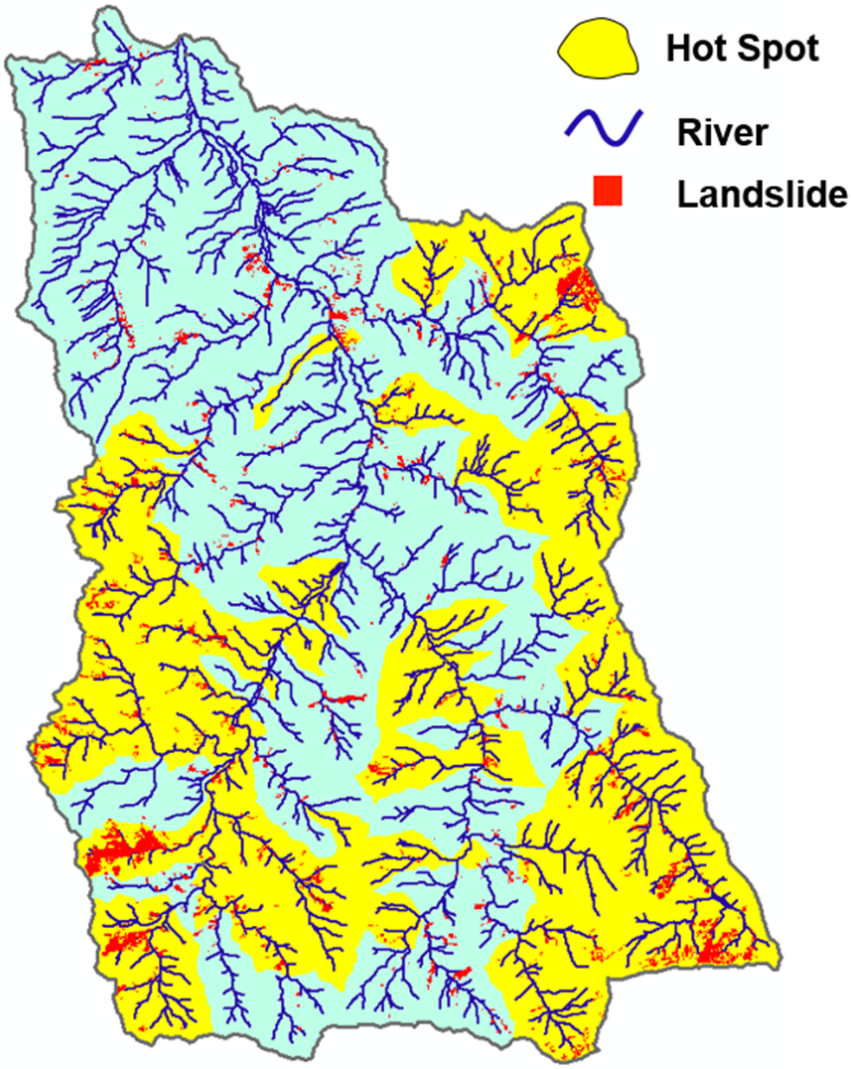

Figure 16. Spatial distribution of actual landslides.

5. CONCLUSION

Based on NCRS-CN, this study investigated the spatial distribution of SY and risk of sediment disaster in typhoon events by using big data collected during 1999–2009. The relationship between potential maximum retention and SY was analyzed and applied to simulate the spatial distribution of the risk of sediment disasters. The results showed that different cumulated rainfall levels, land use, soil, and slope could all be essential factors that affect SY. Based on daily river discharge and SY data, the rating curve (Q–Qs rating curve) of runoff–SY indicated that the coefficient of determination of the curve was $R^2 = 0.95$; thus, the SY of typhoon events can be estimated using the rating curve.

The analytical results of potential maximum retention and SY showed that the relationship between the two parameters could be expressed by a power function. This function could be divided into three categories according to different cumulative rainfall conditions. If the cumulative rainfall was less than 197.2 mm, Type I was applicable, and the SY was 0. If the cumulative rainfall was between 197.2 and 754.4 mm, Type II was applicable, and the corresponding function was $SY = 473.64S^{-0.866}$. If the cumulative rainfall was between 754.4 and 1419.7 mm, Type III was applicable, and the corresponding function was $SY = 13764S^{-1.133}$. The

potential maximum erosion in the catchment area could be estimated using the analytical results of potential maximum retention and SY.

The management strategy of this study was to take management subdivisions as a unit and to use the potential maximum erosion and slope to establish the spatial distribution of sediment disaster risks. The risks were ranked, and the landslide rate of each subdivision was estimated. The results indicated that the cumulative number of subdivision was positively correlated with the landslide rate. In areas with limited data, the relational curve between the cumulative number of subdivisions and landslide rate could be used to determine subdivisions with management priorities. In addition, in the 70% landslide rate simulation scenario, the spatial distribution of landslides in selected subdivisions was mostly consistent with actual landslide locations.

ACKNOWLEDGEMENTS

I would like to express deep and sincere gratitude to my great advisor, Prof. Dr. Chao-Yuan Lin, who teaches me, guide and push me to do research, and mentors me towards academic excellence.

REFERENCES

Ali, M., Khan, S. J., Aslam, I., & Khan, Z. (2011). Simulation of the impacts of land-use change on surface runoff of Lai Nullah Basin in Islamabad, Pakistan. Landscape and Urban Planning, 102(4), 271-279.

Chandramohan, T., Venkatesh, B., & Balchand, A. (2015). Evaluation of three soil erosion models for small watersheds. Aquatic Procedia, 4, 1227-1234.

Chen, C.-S., Jhong, Y.-D., Wu, T.-Y., & Chen, S.-T. (2013). Typhoon event-based evolutionary fuzzy inference model for flood stage forecasting. Journal of Hydrology, 490, 134-143.

Deshmukh, D. S., Chaube, U. C., Hailu, A. E., Gudeta, D. A., & Kassa, M. T. (2013). Estimation and comparision of curve numbers based on dynamic land use land cover change, observed rainfall-runoff data and land slope. Journal of Hydrology, 492, 89-101.

Furl, C., Sharif, H., & Jeong, J. (2015). Analysis and simulation of large erosion events at central Texas unit source watersheds. Journal of Hydrology, 527, 494-504.

Gajbhiye, S., Mishra, S., & Pandey, A. (2014). Relationship between SCS-CN and sediment yield. Applied Water Science, 4(4), 363-370.

Huang, M., Gallichand, J., Wang, Z., & Goulet, M. (2006). A modification to the Soil Conservation Service curve number method for steep slopes in the Loess Plateau of China. Hydrological Processes: An International Journal, 20(3), 579-589.

Jenson, S. K., & Domingue, J. O. (1988). Extracting topographic structure from digital elevation data for geographic information system analysis. Photogrammetric engineering and remote sensing, 54(11), 1593-1600.

Kuo, Y.-C., Lee, M.-A., & Lu, M.-M. (2016). Association of Taiwan's October rainfall patterns with large-scale oceanic and atmospheric phenomena. Atmospheric Research, 180, 200-210.

Lal, M., Mishra, S. K., & Pandey, A. (2015). Physical verification of the effect of land features and antecedent moisture on runoff curve number. Catena, 133, 318-327.

Lee, C.-T. (1996). A geomorphological view to the disaster the chenyulan creek during the herb typhoon. Sino-Geotechnics, 57, 17-24.

Milliman, J., Lee, T., Huang, J., & Kao, S. (2017). Impact of catastrophic events on small mountainous rivers: Temporal and spatial variations in suspended-and dissolved-solid fluxes along the Choshui River, central western Taiwan, during typhoon Mindulle, July 2–6, 2004. Geochimica et Cosmochimica Acta, 205, 272-294.

Mishra, S., Tyagi, J., Singh, V., & Singh, R. (2006). SCS-CN-based modeling of sediment yield. Journal of Hydrology, 324(1-4), 301-322.

Nam, D. H., Kim, M.-I., Kang, D. H., & Kim, B. S. (2019). Debris flow damage assessment by considering debris flow direction and direction angle of structure in South Korea. Water, 11(2), 328.

O'Callaghan, J. F., & Mark, D. M. (1984). The extraction of drainage networks from digital elevation data. Computer vision, graphics, and image processing, 28(3), 323-344.

Oku, Y., & Nakakita, E. (2013). Future change of the potential landslide disasters as evaluated from precipitation data simulated by MRI-AGCM3. 1. Hydrological Processes, 27(23), 3332-3340.

Ozdemir, H., & Elbaşı, E. (2015). Benchmarking land use change impacts on direct runoff in ungauged urban watersheds. Physics and Chemistry of the Earth, Parts A/B/C, 79, 100-107.

Shin, S. S., Park, S. D., Pierson, F. B., & Williams, C. J. (2019). Evaluation of physical erosivity factor for interrill erosion on steep vegetated hillslopes. Journal of Hydrology, 571, 559-572.

Shuin, Y., Hotta, N., Suzuki, M., & Ogawa, K.-i. (2012). Estimating the effects of heavy rainfall conditions on shallow landslides using a distributed landslide conceptual model. Physics and Chemistry of the Earth, Parts A/B/C, 49, 44-51.

Vrieling, A. (2006). Satellite remote sensing for water erosion assessment: A review. Catena, 65(1), 2-18.

Wischmeier, W. H., & Smith, D. D. (1965). Predicting rainfall-erosion losses from cropland east of the Rocky Mountains: Guide for selection of practices for soil and water conservation: Agricultural Research Service, US Department of Agriculture.

Yang, M.-D., Lin, J.-Y., Yao, C.-Y., Chen, J.-Y., Su, T.-C., & Jan, C.-D. (2011). Landslide-induced levee failure by high concentrated sediment flow—A case of Shan-An levee at Chenyulan River, Taiwan. Engineering Geology, 123(1-2), 91-99.

Yang, T.-H., Yang, S.-C., Ho, J.-Y., Lin, G.-F., Hwang, G.-D., & Lee, C.-S. (2015). Flash flood warnings using the ensemble precipitation forecasting technique: A case study on forecasting floods in Taiwan caused by typhoons. Journal of Hydrology, 520, 367-378.

Zanandrea, F., Michel, G. P., Kobiyama, M., & Cardozo, G. L. (2019). Evaluation of different DTMs in sediment connectivity determination in the Mascarada River Watershed, southern Brazil. Geomorphology, 332, 80-87.

Zerihun, M., Mohammedyasin, M. S., Sewnet, D., Adem, A. A., & Lakew, M. (2018). Assessment of soil erosion using RUSLE, GIS and remote sensing in NW Ethiopia. Geoderma regional, 12, 83-90.